# Symmetry-breaking in cumulative measures of shapes of polymer models

Kenneth C. Millett,[1,a)] Eric J. Rawdon,[2,b)] Vy T. Tran,[3,c)] and Andrzej Stasiak[4,d)]
[1]*Department of Mathematics, University of California Santa Barbara, California 93106, USA*
[2]*Department of Mathematics, University of St. Thomas, Saint Paul, Minnesota 55105, USA*
[3]*Department of Physics, Washington University, Saint Louis, Missouri 63130, USA*
[4]*Center for Integrative Genomics, Faculty of Biology and Medicine, University of Lausanne, CH 1015, Switzerland*

(Received 12 July 2010; accepted 9 September 2010; published online xx xx xxxx)

Using numerical simulations we investigate shapes of random equilateral open and closed chains, one of the simplest models of freely fluctuating polymers in a solution. We are interested in the 3D density distribution of the modeled polymers where the polymers have been aligned with respect to their three principal axes of inertia. This type of approach was pioneered by Theodorou and Suter in 1985. While individual configurations of the modeled polymers are almost always nonsymmetric, the approach of Theodorou and Suter results in cumulative shapes that are highly symmetric. By taking advantage of asymmetries within the individual configurations, we modify the procedure of aligning independent configurations in a way that shows their asymmetry. This approach reveals, for example, that the 3D density distribution for linear polymers has a bean shape predicted theoretically by Kuhn. The symmetry-breaking approach reveals complementary information to the traditional, symmetrical, 3D density distributions originally introduced by Theodorou and Suter.
 [doi:10.1063/1.3495482]

## I. INTRODUCTION

Freely jointed equilateral chains provide simple models used to study polymer behavior.[1–19] While one can generate millions of independent configurations and visualize them individually, difficulty arises when one wants to study the aggregation of many configurations to obtain cumulative measures of polymer shape. The cumulative shapes depend on the way the aggregation of the coordinates is accomplished. A conceptually simple approach is to collect coordinates of many independent polymer configurations and then translate the coordinates of each configuration so that their centers of mass coincide with the origin. Using such an approach, the integrated shape of the fluctuating polymer molecules is spherical and its principal characteristic can be expressed by the radius of gyration, revealing the average spatial extension of the modeled chain. Its standard deviation characterizes its fluctuations over time.

A more sophisticated approach is to use the coordinate system based on the three principal axes of inertia determined for each given configuration. The configurations are rotated so that their principal axes of inertia coincide. Such an approach breaks the spherical symmetry and shows that the average shapes of linear polymers can be approximated as prolate ellipsoids.[15,20] Interestingly, for a given form of a polymer (e.g., unbranched linear polymer) and given solvent conditions (e.g., Θ solvent, where the segments of the polymer neither attract nor repel each other), the ratios between the three principal moments of inertia rapidly approach a universal (i.e., independent of the particular chemistry of a given polymer) asymptotic value as the polymer length increases.[21] Although the time-averaged three principal moments of inertia and their respective standard deviations give us a more detailed description of the time-cumulative shapes of polymers, using these measures alone does not reveal how the density of states is distributed within the time-cumulated shapes with ellipsoidal symmetry.

Theodorou and Suter[22] (TS) introduced an approach to investigate the distribution of mass density within accumulated polymer configurations aligned with respect to their three principal axes of rotation. The density distribution was quite complex and showed a low density region around the center of mass of the aggregated configurations. In addition, the three-dimensional density maps obtained by TS are highly symmetric. We know, however, that individual configurations of freely fluctuating polymers are almost never symmetric. Our goal is to construct density maps that reveal this asymmetry. For example, if the TS procedure were applied to aggregate the coordinates of thousands of eggs, the resulting cumulated shape would not resemble an ovoid but rather an ellipsoid since the symmetry along the principal axis would not have been broken. It is relatively simple to align ovoids along their three principal axes of rotation in such a way that the aggregated shape does resemble an ovoid. For example, upon aligning the ovoids along their three principal axes of rotation, one defines the positive principal axis as the direction for which the extension is largest. We have applied this principle of symmetry-breaking in generating three-dimensional (3D) mass density maps of cumulative configurations for six-segment long equilateral chains with four different topologies: linear chains, unknotted circles, and right- and left-handed trefoil knots.

[a)]Electronic mail: millett@math.ucsb.edu.
[b)]Electronic mail: ejrawdon@stthomas.edu.
[c)]Electronic mail: vytran@wustl.edu.
[d)]Electronic mail: andrzej.stasiak@unil.ch.

 

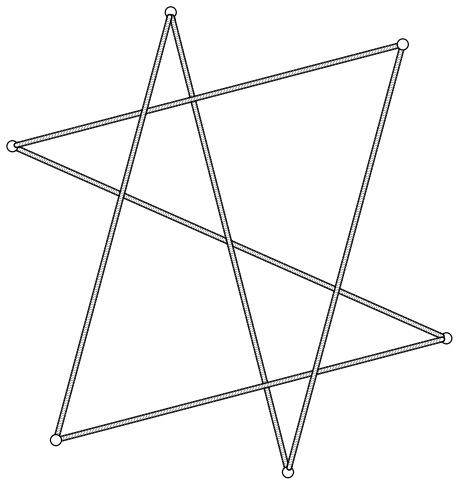

FIG. 1. An equilateral hexagonal trefoil knot in $\mathbb{R}^3$.

## II. DATA GENERATION

The linear chains were generated by joining six random unit vectors. The equilateral hexagonal polygons were sampled using the hedgehog method.[23] In this algorithm an initial configuration is generated by randomly selecting three unit vectors and adding their negatives to give a collection of six unit vectors whose sum is zero. The collection is then subjected to a sequence of independent moves given by randomly selecting two vectors of the six, randomly rotating the vectors about the axis determined by their sum, and replacing the two vectors by the two resulting vectors. These moves have been rigorously proved to be ergodic.[24] The only topological forms that can be produced with six edges are the unknot and left- and right trefoils (see Fig. 1).[25]

The resulting open or closed chain configuration is then rigidly moved to standard position as follows: First one calculates the center of mass of the conformation and translates the configuration so that its center of mass coincides with the origin. Next one determines the three principal axes of rotation assuming that the mass of the polygons is equally redistributed among its vertices. These axes are defined as the eigenvectors of the gyration tensor. Since the gyration tensor is symmetric, the three eigenvectors are mutually orthogonal. The eigenvector corresponding to the largest eigenvalue is aligned with the $x$-axis. Of course, there are two possible orientations, and this is where our work diverges from the work of TS. We choose the positive axis to be the one which gives a positive $x$-coordinate value to the vertex with the highest absolute value of $x$. Next, holding the $x$-axis fixed, one rotates the configuration so that the eigenvector corresponding to the second largest eigenvalue coincides with the $y$-axis and is oriented so that the vertex with the highest absolute value of $y$ has a positive $y$-component. Notice that the orientation of the third eigenvector cannot be changed without also changing the previously selected orientation of the $x$- or $y$-axis. Therefore, the vertex with highest absolute value in the $z$-coordinate may have a positive or negative $z$-value. We call this alignment the *symmetry-breaking alignment* (SBA). In the work of TS, the configurations are aligned so that the principal axes coincide with the coordinate axes, without the additional SBA step of ensuring that the largest $x$- and $y$-values are positive for each configuration.

The final collection of configurations is separated into linear chains, unknotted circles, and right- and left-handed trefoil knots. For the circular chains, the discrimination of individual knot types was achieved by calculating the HOMFLYPT polynomial.[26,27] For each of these four collections, the 3D vertex mass density distributions is determined (assuming unit masses at each of the six vertices). These density distributions determine equidensity surfaces in 3D-space that characterizes the average shape of these four classes of chains.[22] We use a scaling with respect to the maximum density ($\rho_{\max}$) as originally proposed by TS. We consider six such nested surfaces with values $0.03\rho_{\max}$, $0.10\rho_{\max}$, $0.25\rho_{\max}$, $0.35\rho_{\max}$, $0.5\rho_{\max}$, and $0.75\rho_{\max}$, respectively, for each of the types of chains and alignment algorithms.

## III. RESULTS

### A. Effect of symmetry imposing and SBA on linear chains and unknotted circular chains

In Fig. 2, we compare the 3D density distribution of vertices of random six-segment long equilateral linear chains when 1 000 000 independent configurations are aligned along their three principal axes of inertia using the TS method[22] [Fig. 2(a)] and using the SBA method [Fig. 2(b)]. The 3D density distribution is visualized using surfaces that approximate the boundary of the volume enclosing voxels with a given density of vertex points. As these surfaces are nested, we present them separately starting from isodensity surfaces connecting voxels with a low occupation rate (left side of Fig. 2) and ending with the isodensity surfaces joining voxels with a high density of occupation (right side of Fig. 2). In the case of the alignment procedure proposed by TS [Fig. 2(a)] the shapes traced by isodensity surfaces are highly symmetric and show 180° symmetry about the three principal axes and mirror symmetry with respect to the three coordinate planes. These highly symmetric forms were described as *bar of soap* shapes by TS. The SBA procedure leads to a shape with a much lower degree of symmetry although still having a mirror symmetry with respect to $xy$-plane. Interestingly, the shape resembles a bean, as was predicted for random linear chains by Kuhn in 1934.[6] Kuhn used probabilistic arguments to reveal that the average shape of a random polygonal chain breaks the spherical symmetry and can be better approximated by the shape of a bean.

Figure 3 shows the comparison of 3D density distributions for 200 000 independent configurations of unknotted random hexagons when they are aligned using the symmetry imposing (TS) and SBA. Focusing first on the symmetries, we see the same principal features as in Fig. 2, i.e., highly symmetric bar of soap shapes using the TS method and bean shapes with one mirror plane when using the SBA method. With regard to shape descriptors such as the overall size and proportions, we see that the circular chains are more compact than linear chains, as would be expected intuitively. The scale bar on the figures shows the individual segment length.

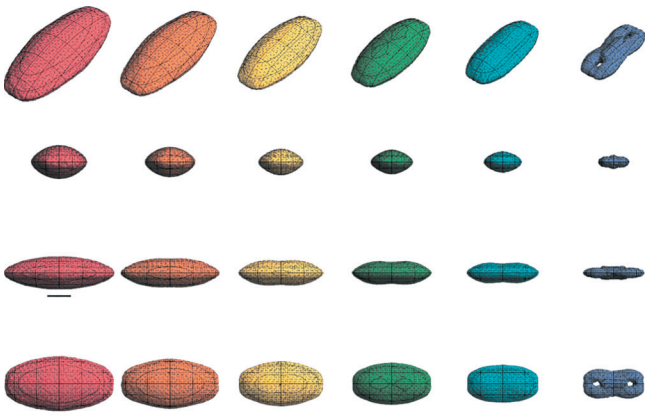

(a) Linear chains - T&S Method

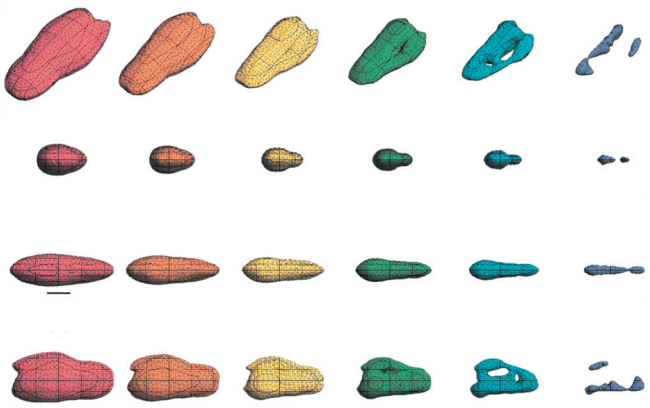

(b) Linear chains - SBA Method

FIG. 2. This figure contains the density isosurfaces for the six-segment long linear chains using the two alignment procedures. The leftmost surfaces engulf the regions with smaller vertex densities and the rightmost surfaces engulf the regions with higher vertex densities. The densities shown are $0.03\rho_{max}$, $0.10\rho_{max}$, $0.25\rho_{max}$, $0.35\rho_{max}$, $0.5\rho_{max}$, and $0.75\rho_{max}$, respectively, where $\rho_{max}$ is the maximum voxel density within this class of chains (linear) using the designated alignment method. The top row shows an angled view followed by a view along each of the three principal axes. The black bar on the left below the third column is the length of one edge segment.

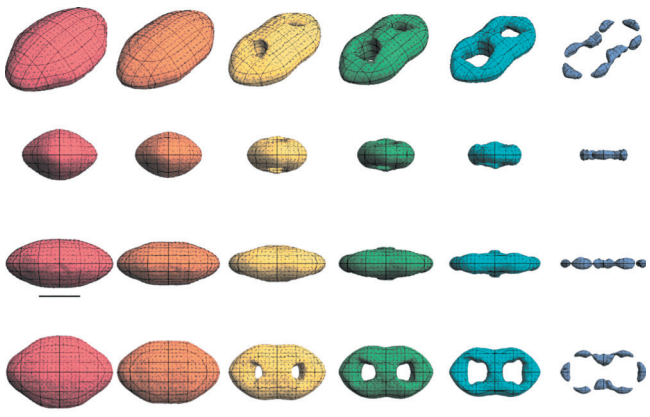

(a) Unknots - T&S Method

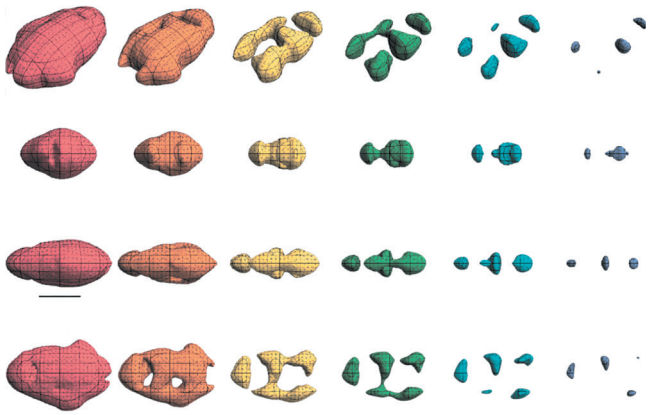

(b) Unknots - SBA Method

FIG. 3. This figure contains the density isosurfaces for the vertex sets of hexagonal unknots. The densities shown are the same as in Fig. 2.

### B. Effect of symmetry imposing and SBA on polygons forming chiral knots

Using the SBA procedure, we decrease the order of symmetry of the surfaces for unknotted random polygons. However, we still have one mirror plane. A natural way of understanding the remaining mirror symmetry is that any configuration of an unknot is as likely as its mirror image. For chiral objects, such as polygons or polymers forming chiral knots, there will be no mirror plane symmetry.

Trefoil knots are chiral and they have right- and left-handed forms that are not topologically interconvertible. We applied the two alignment procedures to see how the chiral nature of random trefoil knot configurations affects the cumulative shapes. Figure 4 compares the 3D density distribution of vertices of random hexagons forming right-handed trefoil knots using the alignment method of TS [Fig. 4(a)] and using the SBA method [Fig. 4(b)]. It is quite apparent that the alignment method of TS produces a 3D density distribution with a high order of symmetry, i.e., having 180° rotational symmetry with respect to each of the three principal axes. Interestingly, despite this symmetry, the aggregated shape is chiral. In Fig. 4(a), the density surfaces are not invariant under mirror reflection through the coordinate planes, which demonstrate their chirality. Note, however, they are invariant under a 180° rotation about the coordinate axes. The SBA images provide strong evidence of this chirality.

Looking at the overall size of surfaces relative to the edge length bars in each image, we see that both alignment procedures (i.e., TS and SBA) reveal that the cumulative shapes of trefoil knots are most compact, followed by surfaces for the unknotted polygons and open chains.

To verify that the symmetry imposing and SBAs are real signatures of chirality in the trefoil configurations, we analyzed the 3D density distributions for hexagons forming left-handed trefoils (see the supplementary materials).[28] Indeed the aggregated shapes are mirror symmetric to those shown in Fig. 4.

AQ: #3

## IV. CONCLUSIONS

We have presented a new method of aligning individual configurations of random chains such as those realized by momentary configurations of thermally fluctuating polymer molecules in a solution. Our method uses the intrinsic asymmetry of individual configurations to specifically orient them along their respective three principal axes of rotation. The SBA alignment procedure performed for random configurations of amphichiral character (i.e., linear and unknotted cy-

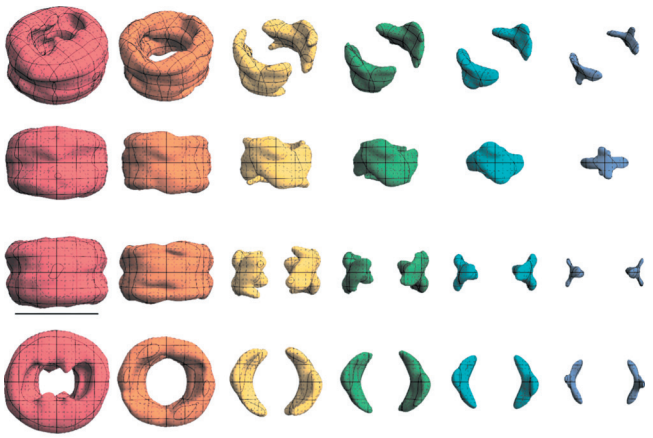

(a) Right-handed trefoils - T&S Method

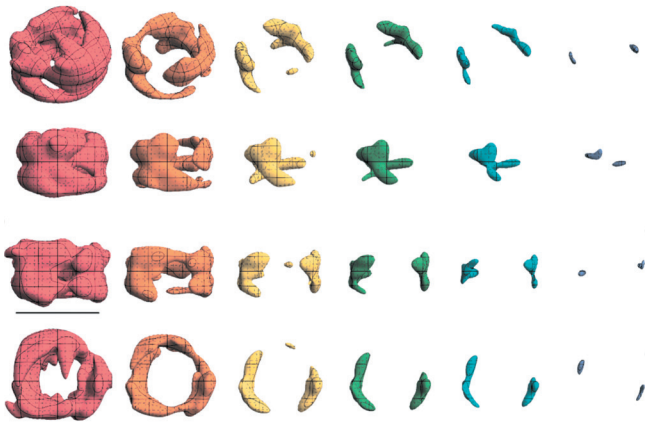

(b) Right-handed trefoils - SBA Method

FIG. 4. This figure contains the density isosurfaces for the hexagonal right-handed trefoils using the two alignment procedures. The densities shown are the same as in Fig. 2. The viewing angle in the first row of Fig. 4(a) may obscure the symmetries in the surfaces. However, the views along the three principal axes of rotation (rows 2–4) clearly show that the cumulative shape obtained using TS alignment method shows 180° rotational symmetry about the center of mass along each of the three principal axes of rotation.

clic chains) reveals a mirror symmetry within the superposed collection of independent configurations. For linear and unknotted circular chains, this mirror symmetry is simply a consequence of the fact that any individual configuration is as likely as its mirror image. However, our alignment method applied to random configurations forming a given chiral knot (with a given handedness) clearly reveals the chiral character of the superposed collection of independent configurations and results in an aggregated shape that is intrinsically asymmetric.

## ACKNOWLEDGMENTS

This material is based upon work supported by the National Science Foundation under Grant No. 0810415 (to E.J.R.) and by the Swiss National Science Foundation under Grant No. 31003A-116275 (to A.S.).

[1] T. Deguchi and K. Tsurusaki, *Series on Knots and Everything*, Lectures at KNOTS '96 (Tokyo) Vol. 15 (World Scientific, Singapore, 1997), pp. 95–122.
[2] A. Dobay, J. Dubochet, K. Millett, P. Sottas, and A. Stasiak, Proc. Natl. Acad. Sci. U.S.A. **100**, 5611 (2003).
[3] A. Dobay, P. Sottas, J. Dubochet, and A. Stasiak, Lett. Math. Phys. **55**, 239 (2001).
[4] A. Y. Grosberg, Macromolecules **41**, 4524 (2008).
[5] K. Koniaris and M. Muthukumar, J. Chem. Phys. **95**, 2873 (1991).
[6] W. Kuhn, Kolloid-Zeitschrift **68**, 2 (1934).
[7] K. C. Millett and E. J. Rawdon, J. Comput. Phys. **186**, 426 (2003).
[8] N. T. Moore and A. Y. Grosberg, Phys. Rev. E **72**, 061803 (2005).
[9] N. T. Moore and A. Y. Grosberg, J. Phys. A **39**, 9081 (2006).
[10] N. T. Moore, R. C. Lua, and A. Y. Grosberg, Proc. Natl. Acad. Sci. U.S.A. **101**, 13431 (2004).
[11] N. T. Moore, R. C. Lua, and A. Y. Grosberg, *Series on Knots and Everything*, Physical and Numerical Models in Knot Theory Vol. 36 (World Scientific, Singapore, 2005), pp. 363–384
[12] R. C. Lua, N. T. Moore, and A. Y. Grosberg, *Series on Knots and Everything*, Physical and Numerical Models in Knot Theory Vol. 36 (World Scientific, Singapore, 2005), pp. 385–398.
[13] A. A. Podtelezhnikov, N. R. Cozzarelli, and A. V. Vologodskii, Proc. Natl. Acad. Sci. U.S.A. **96**, 12974 (1999).
[14] E. J. Rawdon, A. Dobay, J. C. Kern, K. C. Millett, M. Piatek, P. Plunkett, and A. Stasiak, Macromolecules **41**, 4444 (2008).
[15] E. J. Rawdon, J. C. Kern, M. Piatek, P. Plunkett, A. Stasiak, and K. C. Millett, Macromolecules **41**, 8281 (2008).
[16] S. Y. Shaw and J. C. Wang, Science **260**, 533 (1993).
[17] M. K. Shimamura and T. Deguchi, J. Phys. A **35**, L241 (2002).
[18] A. Stasiak, V. Katritch, J. Bednar, D. Michoud, and J. Dubochet, Nature (London) **384**, 122 (1996).
[19] A. V. Vologodskii, N. J. Crisona, B. Laurie, P. Pieranski, V. Katritch, J. Dubochet, and A. Stasiak, J. Mol. Biol. **278**, 1 (1998).
[20] K. C. Millett, P. Plunkett, M. Piatek, E. J. Rawdon, and A. Stasiak, J. Chem. Phys. **130**, 165104 (2009).
[21] J. Rudnick and G. Gaspari, J. Phys. A **19**, L191 (1986).
[22] D. N. Theodorou and U. W. Suter, Macromolecules **18**, 1206 (1985).
[23] K. V. Klenin, A. V. Vologodskii, V. V. Anshelevich, A. M. Dykhne, and M. D. Frank-Kamenetskii, J. Biomol. Struct. Dyn. **5**, 1173 (1988).
[24] S. Alvarado, J. A. Calvo, and K. C. Millett, Preprint (2010).
[25] R. Randell, J. Knot Theory Ramif. **3**, 279 (1994).
[26] P. Freyd, D. Yetter, J. Hoste, W. B. R. Lickorish, K. Millett, and A. Ocneanu, Bull., New Ser., Am. Math. Soc. **12**, 239 (1985).
[27] J. H. Przytychki and P. Traczyk, Kobe J. Math. **4**, 115 (1988).
[28] See supplementary material at http://dx.doi.org/10.1063/1.3495482 for a comparison of the density isosurfaces for right- and left-handed trefoil knots using the TS and SBA methods.

## AUTHOR QUERIES — 054037JCP

#1 Au: References are cited out of order. Please check the renumbering of references.
#2 Au: Please use the spelled-out form of HOMFLYPT, if possible and acronym not commonly known to your readers.
#3 Au: Reference 27 was added in the reference list as epaps. Please check.
#4 Au: Please check the book title in Refs. 2, 15, and 16.
#5 Au: Please check the journal title in Refs. 6 and 26.